International Journal of Thermophysics, Vol. 12, No. 6, 1991

Thermal Conductivity Surface of Argon: A Fresh Analysis

R. A. Perkins,[1] D. G. Friend,[1] H. M. Roder,[1] and C. A. Nieto de Castro[2,3]

Received March 21, 1991

This paper presents a fresh analysis of the thermal conductivity surface of argon at temperatures between 100 and 325 K with pressures up to 70 MPa. The new analysis is justified for several reasons. First, we discovered an error in the compression-work correction, which is applied when calculating thermal conductivity and thermal diffusivity obtained with the transient hot-wire technique. The effect of the error is limited to low densities, i.e., for argon below 5 mol · L^{-1}. The error in question centers on the volume of fluid exposed to compression work. Once corrected, the low-density data agree very well with the available theory for both dilute-gas thermal conductivity and the first density coefficient of thermal conductivity. Further, the corrected low-density data, if used in conjunction with our previously reported data for the liquid and supercritical dense-gas phases, allow us to represent the thermal conductivity in the critical region with a recently developed mode-coupling theory. Thus the new surface incorporates theoretically based expressions for the dilute-gas thermal conductivity, the first density coefficient, and the critical enhancement. The new surface exhibits a significant reduction in overall error compared to our previous surface which was entirely empirical. The uncertainty in the new thermal conductivity surface is ±2.2% at the 95% confidence level.

KEY WORDS: argon; liquid; supercritical; surface fit; thermal conductivity; transient hot wire technique; vapor.

1. INTRODUCTION

We have studied the thermal conductivity of argon extensively using the transient hot-wire technique [1–5]. In our previous paper [5], we recom-

[1] Thermophysics Division, National Institute of Standards and Technology, Boulder, Colorado 80303, U.S.A.

[2] Departamento de Quimica, Faculdade de Ciencias, Universidade de Lisboa, 1700 Lisboa, Portugal.

[3] Centro de Quimica Estrutural, Complexo I, IST, 1096 Lisboa Codex, Portugal.

840/12/6-2

0195-928X/91/1100-0965$06.50/0 © 1991 Plenum Publishing Corporation

mended that a new effort be undertaken to correlate the thermal conductivity of argon at low temperatures. This paper presents the results of such an effort. While comparing our argon data to recent theories for the dilute-gas thermal conductivity, λ_0, and the first density coefficient of thermal conductivity, λ_1, we discovered an error in the compression-work correction which is applied when calculating thermal conductivity and thermal diffusivity. The effect of the error is limited to low densities, i.e., below 5 mol $\cdot$ L^{-1} for argon. The error in question centers on the volume of fluid exposed to compression work and is described in detail in Section 2. We present corrected values for the thermal conductivity and thermal diffusivity of argon at densities below about 5 mol $\cdot$ L^{-1} in Section 3. We show that the revised low-density values are in good agreement with the theories for both λ_0 and λ_1 in Section 4. The corrected low-density data, if used in conjunction with our previously reported data for the liquid and supercritical dense-gas phases, allow us to represent the thermal conductivity in the critical region with a recently developed mode-coupling theory as discussed in Section 5. Finally, the development of the new thermal conductivity surface is given in Section 6.

2. COMPRESSION-WORK CORRECTION

The transient hot-wire technique is widely accepted as an accurate method for measuring the thermal conductivity of fluids. The working equation for the temperature rise at the surface of an idealized wire is given by

$$\Delta T_{\mathrm{id}}(r_0, T) = \frac{q}{4\pi\lambda} \ln\left(\frac{4at}{r_0^2 C}\right) = \frac{q}{4\pi\lambda} \ln\left(\frac{4a}{r_0^2 C}\right) + \frac{q}{4\pi\lambda} \ln(t) \tag{1}$$

In Eq. (1), q is the power input per unit length of wire, t is the elapsed time from the start of a step power input, λ is the fluid thermal conductivity, $a = \lambda/\rho C_{\mathrm{p}}$ is the fluid thermal diffusivity, r_0 is the radius of the wire, ρ is the fluid density, C_{p} is the fluid isobaric heat capacity, and C is the exponential of Euler's constant. Using Eq. (1), we obtain the thermal conductivity from the slope of a line fit through the temperature rise versus $\ln(t)$. The thermal diffusivity is obtained from the intercept of this line.

The ideal temperature rise is obtained by adding a number of temperature rise corrections to the experimental temperature rise:

$$\Delta T_{\mathrm{id}} = \Delta T_{\mathrm{exp}} + \sum_i \delta T_i \tag{2}$$

These temperature rise corrections account for heat transfer mechanisms other than one-dimensional radial heat conduction from an infinite line

source. These corrections are described in Refs. 6 and 7. The most significant correction accounts for the finite heat capacity of the platinum hot wire [7]. We found that there was an error in our implementation of the correction which accounts for fluid compression work. This error was due to an ambiguous definition in Ref. 6 of the volume over which the compression work is done.

The compression-work correction was originally developed by Healy et al. [6]. The effect of the fluid compression-work correction on the thermal diffusivity has been investigated by Nieto de Castro et al. [7]. The temperature rise associated with the compression-work correction, δT_3, in the notation of Ref. 7, is approximated by

$$\delta T_3(t) = \frac{\Delta P(t)}{\rho C_p} \tag{3}$$

where ΔP is the pressure change due to heating the system. The pressure rise and δT_3 are assumed to have no spatial dependence and must propagate through the entire system volume, V. The calculation of ΔP proceeds by assuming ideal-gas thermodynamics. The temperature change in the fluid causes both spatial and temporal variations of the fluid density. We can use the conservation of mass and integrate over the entire system volume to obtain an expression for $\Delta P(t)$. We then use Eq. (3) and perform the integration over the position-independent terms in the temperature field, δT_3, and the initial cell temperature. After solving for δT_3, we have

$$\delta T_3(t) = \frac{R}{C_v V} \int_v \Delta T(r, t)\, dV \tag{4}$$

where C_v is the fluid isochoric heat capacity, R is the gas constant, and $\Delta T(r, t)$ is the position-dependent contribution to the temperature field.

To evaluate Eq. (4), we need an expression for $\Delta T(r, t)$. The most straightforward approximation, used in both Ref. 6 and Ref. 7, is to use the cylindrically symmetrical solution of the idealized differential equation for a line source of heat with boundary conditions specified in Ref. 6. This solution looks similar to Eq. (1), except that the factor $\ln[4at/(r_0^2 C)]$ is replaced by $E_1[r^2/(4at)]$, where E_1 is the exponential integral and r is the radial distance. When all temperature corrections are sufficiently small, this expression for $\Delta T(r, t)$ should be a valid approximation to lowest order. The volume integral of Eq. (4) is converted to a one-dimensional integral with the radial distance varying between r_0 and b, the radii of the cylindrical cavities containing the hot wires. The axial length for which this solution is appropriate is the length over which heat is applied, i. e., the total

length L of the long and short hot wires. Thus, Healy et al. [6] equated the volume V with the volume of the cylindrical cavity with height L. This volume has always been used previously in our data analysis procedure.

However, the pressure pulse clearly propagates throughout the cell volume; our pressure transducer indicates this process. The compression work is done on the entire volume containing the fluid, and the mass conservation equation must be applied to this larger volume. It seems clear, then, that V in Eq. (4) represents the entire volume which contains the fluid sample. We cannot easily calculate the temperature field $\Delta T(r, t)$ in the external fluid-filled volumes. These volumes consist of relatively small-gauge volumes and capillaries, whose temperature ranges up to room temperature, and larger volumes near the cell temperature, including the head spaces surrounding the top and bottom wire suspensions and a cylindrical cavity coaxial with the short hot wire but containing no heating element. For these volumes, we set $\Delta T(r, t) = 0$. This assumption, implicitly made in Ref. 7, is certainly not correct, but provides a useful approximation. Our expression for $\delta T_3(t)$, to lowest (zeroth) order in the small quantity $r_0^2/4at$, is

$$\delta T_3(t) = -\frac{qLRt}{\rho C_p C_v V}\left[1 - \exp\left(\frac{-b^2}{4at}\right) + \frac{b^2 \rho C_p}{4\lambda t} E_1\left(\frac{b^2}{4at}\right)\right] \tag{5}$$

Our Eq. (5) agrees with the result from Ref. 7, except that the factor of b^2L was inadvertently equated to the system volume in Eq. (15) of Ref. 7.

The expression for the compression-work correction in Ref. 6 is identical to the first term in Eq. (5); the other terms in Eq. (5) are generally negligible for our cell at all accessible thermodynamic conditions. The use of the volume of the cylindrical cavity, $\pi b^2 L$, for V led to a serious overestimation of the contribution of δT_3 to the measured temperature rise of the hot wire. The correction for the compression work becomes more significant as the fluid density decreases. In addition, it is apparent that the correction is more significant for fluids with small heat capacities. The heat capacities of the polyatomic molecules which we have studied in the past are larger than those of monatomic molecules such as argon. Since the magnitude of this correction is smaller for polyatomic molecules, we did not detect significant errors during our previous studies of polyatomic gases. Argon is the only fluid for which we have been able to detect significant error due to the fluid compression-work correction over the density range which we have reported.

Even though the fluid compression-work correction is derived for the cavity volume in Ref. 6, the authors point out that the temperature rise can be affected by connecting an external volume to the hot-wire cell. This

implies that they considered the total volume containing the fluid sample to be a critical parameter in assessing the compression-work correction. The total volume of the vessel is explicitly used in Ref. 7, and increasing the fluid volume is again suggested as a method of evaluating the calculation of δT_3. It is also suggested that the calculation of δT_3 is not sufficiently accurate for direct application to experimental temperature rises but, rather, that conditions where this correction is significant should be avoided. Based on our reanalysis of the compression-work correction, we conclude that the volume used in Eq. (5) should be the total cell volume and not the cavity volume which we have previously used. We have not addressed the various assumptions, such as insulated boundary conditions at the fluid–wall interface, which may lead to additional errors in this temperature-rise correction.

The total volume of our transient hot-wire cell is 27.86 cm^3. Since we have been using the cavity volume of 9.89 cm^3, the correction for fluid compression work which we used was 2.8 times too large. For argon near 103 K and 0.2 $mol \cdot L^{-1}$, at a point with a temperature rise of about 2.2 K (about 400 ms from the start of the heating pulse), the old compression-work term contributed about 0.014 K or 0.6%. With the more appropriate value of V, the compression-work term becomes about 0.0048 K or 0.2%. The second term in Eq. (5) is about 0.2×10^{-6} K, and the third term is about 0.2×10^{-8} K; these terms remain unimportant for our calculations. Our previous implementation of the compression-work correction leads to a measured thermal conductivity which is 6% too high for the subcritical vapor. Under these conditions the erroneous compression-work correction leads to a measured heat capacity which is 25% too small. The compression-work correction has significantly altered both the slope and the intercept of the temperature rise versus log time curve under these conditions. When we reanalyze the argon data under these conditions using the total cell volume, we obtain heat capacity data which agree well with equation-of-state predictions. Therefore, we conclude that we have a better energy balance when we use the total cell volume in the fluid compression-work correction. No difference in the thermal conductivity or thermal diffusivity of argon is obtained at densities above 5 $mol \cdot L^{-1}$.

3. CORRECTED LOW-DENSITY RESULTS

Since there is no difference in the thermal conductivity data at higher densities, we report only the altered data points at densities below 5 $mol \cdot L^{-1}$. The corrected low-density results are provided in Table I. These values supercede the values presented by Roder et al. [5]. Some additional data points are included in Table I which were not presented by

Table I. The Corrected Thermal Conductivity, Thermal Diffusivity, and Heat Capacity of Argon at Densities Less than 5 mol · L^{-1}

Cell pressure P (MPa)	Nominal density $\rho_n(T_n, P)$ (mol · L^{-1})	Thermal conductivity $\lambda_n(T_n, \rho_n)$ (W · m^{-1} · K^{-1})	Thermal diffusivity $[10^9 \cdot \alpha(T_n, \rho_n)]$ ($m^2 \cdot s^{-1}$)	Heat capacity $C_p(T_n, \rho_n)$ (J · mol^{-1} · K^{-1})
		Nominal Temperature, 103 K		
0.271	0.336	0.00676	816.9	24.6
0.193	0.236	0.00666	1209.1	23.4
		Nominal temperature, 113 K		
0.636	0.760	0.00782	356.8	28.8
0.458	0.528	0.00754	597.4	23.9
0.297	0.332	0.00734	978.3	22.6
		Nominal temperature, 123 K		
1.157	1.355	0.00920	207.7	32.7
0.852	0.942	0.00861	330.3	27.7
0.598	0.635	0.00823	510.8	25.4
0.343	0.350	0.00796	973.5	23.3
		Nominal temperature, 133 K		
2.014	2.422	0.01130	106.5	43.8
1.690	1.904	0.01051	176.5	31.3
1.400	1.502	0.00987	234.8	28.0
1.150	1.189	0.00946	313.6	25.4
0.885	0.882	0.00911	439.1	23.5
0.587	0.564	0.00877	711.8	21.8
0.286	0.266	0.00851	1613.6	19.8
		Nominal temperature, 142 K		
2.988	3.755	0.01469	68.3	57.3
2.577	2.961	0.01272	97.5	44.0
2.244	2.433	0.01172	126.0	38.2
1.853	1.899	0.01083	175.2	32.6
1.476	1.442	0.01024	249.9	28.4
1.159	1.093	0.00983	339.3	26.5
0.842	0.768	0.00950	514.2	24.0
0.446	0.392	0.00915	1065.3	21.9

Table I. *(Continued)*

Cell pressure P (MPa)	Nominal density $\rho_n(T_n, P)$ (mol · L^{-1})	Thermal conductivity $\lambda_n(T_n, \rho_n)$ (W · m^{-1} · K^{-1})	Thermal diffusivity $[10^9 \cdot \alpha(T_n, \rho_n)]$ (m^2 · s^{-1})	Heat capacity $C_p(T_n, \rho_n)$ (J · mol^{-1} · K^{-1})
		Nominal temperature, 157 K		
4.153	4.698	0.01629	69.5	49.9
3.825	4.117	0.01511	88.4	41.5
3.385	3.439	0.01389	111.7	36.2
3.060	2.995	0.01322	133.9	33.0
2.650	2.485	0.01244	172.5	29.0
2.336	2.126	0.01198	206.4	27.3
1.732	1.497	0.01120	310.0	24.1
1.225	1.018	0.01068	424.6	24.7
		Nominal temperature, 173 K		
5.082	4.835	0.01680	102.8	33.8
4.800	4.460	0.01618	111.2	32.6
4.453	4.024	0.01548	113.3	34.0
4.008	3.502	0.01470	134.6	31.2
3.573	3.028	0.01402	154.4	30.0
3.092	2.538	0.01335	202.3	26.0
2.607	2.076	0.01280	260.7	23.6
1.933	1.481	0.01215	366.4	22.4
1.352	1.004	0.01165	529.9	21.9
0.974	0.710	0.01144	806.1	20.0
0.500	0.356	0.01124	1827.9	17.3
0.293	0.206	0.01121	3506.2	15.5
		Nominal temperature, 203 K		
6.107	4.372	0.01733	138.8	28.6
5.659	3.990	0.01683	151.6	27.8
4.876	3.351	0.01599	182.0	26.2
4.392	2.970	0.01553	219.9	23.8
3.548	2.336	0.01480	285.1	22.2
2.870	1.850	0.01430	365.8	21.1
2.240	1.416	0.01387	469.9	20.8
1.255	0.771	0.01325	884.6	19.4

Table I. *(Continued)*

Cell pressure P (MPa)	Nominal density $\rho_n(T_n, P)$ (mol · L^{-1})	Thermal conductivity $\lambda_n(T_n, \rho_n)$ (W · m^{-1} · K^{-1})	Thermal diffusivity $[10^9 \cdot \alpha(T_n, \rho_n)]$ (m^2 · s^{-1})	Heat capacity $C_p(T_n, \rho_n)$ (J · mol^{-1} · K^{-1})
		Nominal temperature, 223 K		
7.705	4.874	0.01904	155.3	25.2
6.951	4.332	0.01835	173.3	24.4
6.356	3.913	0.01778	182.9	24.8
5.711	3.470	0.01723	203.3	24.4
5.035	3.016	0.01669	224.0	24.7
4.338	2.561	0.01614	275.8	22.9
3.519	2.042	0.01560	324.3	23.6
2.699	1.539	0.01507	430.7	22.7
1.985	1.115	0.01469	626.2	21.0
0.864	0.474	0.01420	1520.9	19.7
		Nominal temperature, 274 K		
9.224	4.350	0.02103	182.1	26.6
7.434	3.467	0.02001	234.8	24.6
5.954	2.748	0.01918	294.3	23.7
4.596	2.099	0.01849	382.7	23.0
3.266	1.476	0.01797	568.3	21.4
1.884	0.841	0.01734	942.8	21.9
1.353	0.601	0.01719	1407.5	20.3
0.569	0.251	0.01704	3708.2	18.3
		Nominal temperature, 302 K		
10.974	4.575	0.02278	196.8	25.3
9.573	3.978	0.02197	222.0	24.9
7.851	3.245	0.02112	263.1	24.7
6.313	2.595	0.02046	347.7	22.7
4.432	1.807	0.01955	462.7	23.4
2.849	1.152	0.01888	752.0	21.8
0.926	0.371	0.01815	2554.7	19.2
		Nominal temperature, 324 K		
11.400	4.349	0.02354	207.9	26.0
8.691	3.306	0.02246	265.6	25.6
7.537	2.862	0.02191	319.8	23.9
5.306	2.004	0.02094	443.8	23.5
3.709	1.395	0.02025	600.2	24.2
2.367	0.886	0.01987	991.6	22.6
1.343	0.501	0.01965	1862.4	21.1

Roder et al. [5]. These points are at densities below 1 mol · L^{-1} and were omitted in the original analysis since they deviated by several percent from the high-density data along a given isotherm. Proper application of the compression-work correction now allows us to report argon thermal conductivities down to densities as low as 0.2 mol · L^{-1}. Each reported data point is the average of four data points at varying power levels. The revised values for thermal diffusivity and heat capacity at low densities are in much better agreement with equation-of-state predictions. We estimate that the uncertainty in the thermal conductivity data reported in Table I is $\pm 1\%$ and the uncertainty in the heat capacity is $\pm 5\%$ except at the lowest densities.

Our thermal conductivity data have been adjusted to nominal isotherm temperatures. This adjustment is made with the surface fit described in this paper. We have used temperatures on the IPTS-68 scale throughout this work for consistency with our previous studies. The equation of state of Younglove [8] is used to obtain the densities reported in Table I. In addition, this equation of state provides the isobaric heat capacity values which are used to adjust the experimental thermal diffusivity and heat capacity values to the nominal isotherm temperatures. An improved equation of state has recently been reported by Stewart and Jacobsen [9] which is more accurate in the critical region. We have not observed significant differences in the densities calculated with the two equations of state far from the critical region, so we have continued to use the Younglove [8] equation of state to be consistent with the previously reported densities. However, we have observed significant differences in the compressibilities and in the heat capacities predicted by the two equations of state in the critical region. We have, therefore, used the equation of state of Stewart and Jacobsen [9] in our present analysis of the critical enhancement using mode-coupling theory.

4. LOW-DENSITY ANALYSIS

Our corrected low-density thermal conductivity data are adjusted to nominal isotherm temperatures. These data are fitted to a linear function with respect to density for each isotherm. This fit provides the dilute-gas thermal conductivity λ_0 as the intercept and the first density coefficient of thermal conductivity λ_1 as the slope. The results of this fit are presented in Table II.

Figure 1 shows deviations among our new dilute-gas λ_0 data several correlations [10–13], and the other available data [14, 15, 16, 17, 19, 20]. Kestin et al. [10] have presented a comprehensive corresponding states correlation for the dilute-gas thermal conductivity λ_0 of noble gases

Table II. Dilute-Gas Thermal Conductivity λ_0(exp) and First Density Coefficient of Thermal Conductivity λ_1(exp), Obtained by Linear Regression of Low-Density Data up to a Maximum Density of ρ_{max}[a]

T (K)	$mW \cdot m^{-1} \cdot K^{-1}$		$mW \cdot L \cdot mol^{-1} \cdot m^{-1} \cdot K^{-1}$		ρ_{max} ($mol \cdot L^{-1}$)
	λ_0(exp)	λ_0(calc)	λ_1(exp)	λ_1(calc)	
103.00	6.42	6.38	1.00	1.05	0.340
113.00	7.00	6.98	1.03	1.05	0.525
123.00	7.57	7.60	1.08	1.05	0.952
133.00	8.18	8.23	1.09	1.05	1.523
142.00	8.69	8.81	1.10	1.06	1.909
157.00	9.56	9.77	1.05	1.06	1.478
173.00	10.63	10.77	1.06	1.07	2.517
203.00	12.39	12.57	1.06	1.07	3.339
223.00	13.43	13.73	1.08	1.07	3.475
273.00	16.41	16.45	1.00	1.06	3.489
302.00	17.70	17.93	1.06	1.05	3.988
324.00	18.89	19.02	1.06	1.05	4.351

[a] λ_0(calc) is from Kestin et al. [10], and λ_1(calc) is from Rainwater and Friend [22].

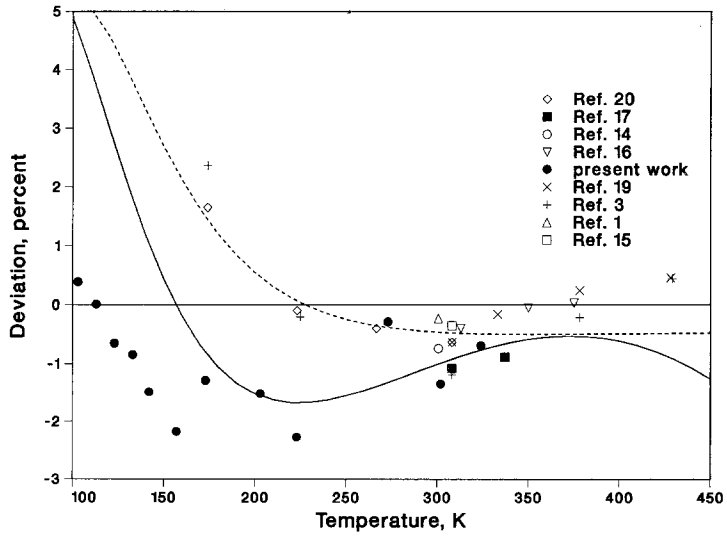

Fig. 1. Deviations between the experimental dilute gas thermal conductivity, λ_0, of argon and the correlation of Kestin et al. [10] as a function of temperature. Dashed line shows deviations with the correlation of Rabinovich et al. [13]. Solid line shows deviations with the correlation of Trappeniers [12].

and their mixtures. This correlation is consistent for both equilibrium and transport properties over a wide range of temperature. Younglove and Hanley [11] provide a simple polynomial fit for λ_0 of argon which reproduces the Kestin et al. [10] dilute-gas λ_0 function almost exactly.[4] The dilute-gas function of Kestin et al. [10] is selected as the baseline for the deviation plot in Fig. 1.

The most recent and comprehensive treatment of the first density coefficient of thermal conductivity has been given by Rainwater and Friend [21, 22]. We restrict our comparisons to their model, which includes two-monomer, three-monomer, and monomer-dimer contributions. Nieto de Castro et al. [23] have shown that this theory is a good representation of the first density coefficient for both monatomic and polyatomic molecules over a wide range of temperature. These authors [21–23] define a reduced thermal conductivity virial coefficient b_λ by

$$b_\lambda = \frac{3B_\lambda}{2\pi N_A \sigma^3} \tag{6}$$

where $B_\lambda = \lambda_1/\lambda_0$, N_A is Avogadro's number, and σ is the Lennard–Jones molecular diameter. The reduced thermal conductivity virial coefficient is a universal function of reduced temperature for a given interaction potential for monatomic gases; Ref. 23 discusses the application to polyatomic fluids. The reduced temperature ($T^* = k_B T/\varepsilon$) is defined in terms of the Lennard–Jones energy parameter ε and the Boltzmann constant k_B.

Figure 2 shows our new experimental thermal conductivity data along isotherms as well as lines which are defined by

$$\lambda(\text{calc}) = \lambda_0(K) + \lambda_1(RF)\,\rho \tag{7}$$

where $\lambda_0(K)$ is taken from Ref. 10, and $\lambda_1(RF)$ is from Ref. 22. The calculated values for λ_0 and λ_1 are tabulated for each isotherm in Table II. Figure 2 shows that the theoretically based expressions for λ_0 and λ_1 are in good agreement with our revised experimental data. The discussion on page 1158 in Ref. 5 can now be completed, namely, once the fluid compression-work correction was modified, our experimental results agree with the extended law of corresponding states of Kestin et al. [10] to within 2% at temperatures between 103 and 324 K. Although slightly different curvatures are found for the experimental data and the theoretical predictions, our revised results confirm the correlation of Kestin et al. [10] within 2%.

[4] For the remainder of the paper whenever we refer to the dilute-gas function of Kestin et al. [10], we mean the dilute-gas function of Kestin et al. [10] as approximated by the polynomial of Younglove and Hanley [11].

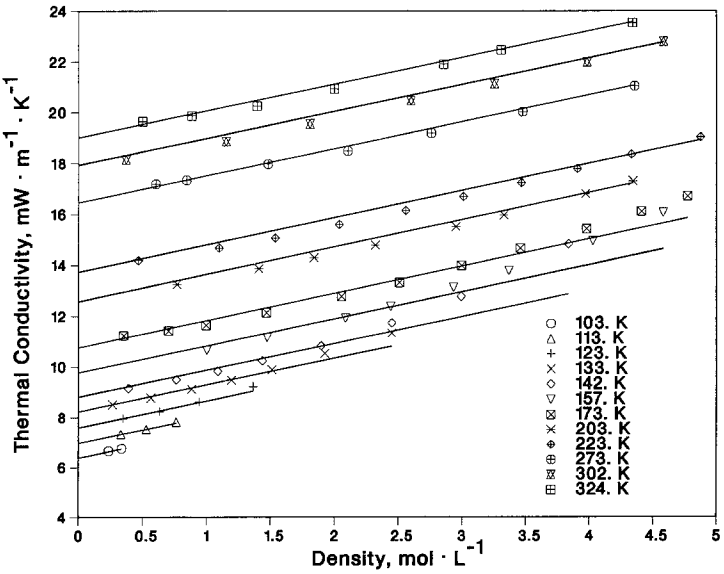

Fig. 2. The low-density thermal conductivity of argon. Lines are given by $\lambda = \lambda_0 + \lambda_1 \rho$, where λ_0 is from Kestin et al. [10] and λ_1 is from Rainwater and Friend [21, 22].

5. CRITICAL ENHANCEMENT

A theory describing the divergence of the thermal conductivity in the asymptotically critical region has been well developed for pure fluids [24]. More recently, Olchowy and Sengers have proposed a solution to the mode-coupling equations which allows calculation of the thermal conductivity enhancement throughout the fluid state [25]; a simplified version of this theory, which incorporates an ad hoc procedure and approximates the full theory, has also been published [26]. The theory has been used successfully to describe transport data of carbon dioxide, methane, ethane, helium 3, and water [25–29].

The approach involves the approximate solution of coupled integral equations with a wave number cutoff (q_D) to limit the momentum-space range over which critically driven fluctuations can contribute to dynamic critical phenomena. Thus, in addition to a knowledge of thermodynamic properties and background values of the viscosity and thermal conductivity, the single fluid-dependent parameter q_D must be fitted to describe the critical enhancement contribution. In this work, we have used the classical argon equation of state and critical parameters of Stewart and Jacobsen [9], the fluid-dependent equilibrium critical amplitudes of

Sengers et al. [24], and the scaling law exponents of Olchowy and Sengers [25]. Because none of our data are in the asymptotically critical region, we do not need a scaling-law equation of state, and the viscosity η, which has a much weaker critical enhancement than the thermal conductivity, can be well approximated by its background contribution. This viscosity is calculated with the function of Younglove and Hanley [11].

The thermal conductivity enhancement can be described by [25]

$$\Delta\lambda_{cr} = \frac{R_c k_B T \rho C_p}{6\pi\eta\xi}(\Omega - \Omega_0) \tag{8}$$

where the amplitude R_c has been set to 1.01, k_B is Boltzmann's constant, ξ is the correlation length, and Ω and Ω_0 are complicated functions of T and ρ as briefly described below.

The correlation length ξ has been approximated by relating it to the critical part of the dimensionless compressibility as in Refs. 25–29. Thus, we write

$$\xi = \xi_0 \left[\frac{P_c \rho}{\Gamma \rho_c^2}\right]^{(\nu/\gamma)} \left[\left.\frac{\partial\rho(\rho, T)}{\partial P}\right|_T - \left(\frac{T_r}{T}\right)\left.\frac{\partial\rho(\rho, T_r)}{\partial P}\right|_T\right]^{(\nu/\gamma)} \tag{9}$$

In Eq. (9) ν and γ are universal scaling exponents, while Γ and ξ_0 are fluid specific amplitudes. The temperature at which the background compressibility has been identified with the total compressibility, so that the critical contribution vanishes, is not well defined. This temperature T_r is well above the critical temperature and has variously been defined as $1.5T_c$, approximately $2T_c$, and $2T_c$ in Refs. 25–29. Because our argon data clearly indicate an enhancement for isotherms above $2T_c$ (303 K), we have increased the value of T_r to $2.5T_c$. The correlation length for critical fluctuations, and hence the critical enhancement, vanishes above this temperature; thus, both ξ in Eq. (7) and $\Delta\lambda_{cr}$ in Eq. (8) should be set to 0 for temperatures above $2.5T_c$. The choice of T_r is arbitrary, and affects the calculated enhancement only at temperatures well above the critical temperature.

The function Ω in Eq. (8) can be evaluated using the parameters

$$y_D = q_D \xi \tag{10a}$$

$$y_\gamma = C_v/(C_p - C_v) \tag{10b}$$

$$y_\alpha = (k_B T M \rho)/(8\pi\eta^2\xi) \tag{10c}$$

$$y_\beta = [(\lambda_0 + \lambda_{ex})\, M]/[\eta(C_p - C_v)] \tag{10d}$$

and

$$y_\delta = \{\tan^{-1}[q_D\xi/(1 + q_D^2\xi^2)^{1/2}] - \tan^{-1}(q_D\xi)\}/(1 + q_D^2\xi^2)^{1/2} \tag{10e}$$

where M is the molar mass and the other variables have been defined above. The final expression for Ω from Refs. 25, 26, and 28 has been simplified [29, 30] by evaluating the mode-coupling integral in closed algebraic form; the matrix-inversion algorithm, required to use the results reported by Sengers and Olchowy [25, 26, 28], is no longer necessary. We can write

$$\Omega = \frac{2}{\pi(1+y_\gamma)}\left[y_D + \sum_{i=1}^{4}\left[\frac{g(z_i)(1-z_i^2)^{-1/2}}{\prod_{i\neq j=1}^{4}(z_i - z_j)} \times \ln\left(\frac{1 - z_i + (1-z_i^2)^{1/2}\tan^{-1}\left(\frac{y_D}{2}\right)}{1 - z_i - (1-z_i^2)^{1/2}\tan^{-1}\left(\frac{y_D}{2}\right)} \right) \right] \right] \tag{11}$$

The auxiliary function $g(z)$ is defined by

$$g(z) = -y_D y_\alpha z^3 + (y_\gamma - y_\beta - y_\alpha y_\delta) z^2 - y_\gamma y_D y_\alpha z + y_\gamma^2 - y_\gamma y_\delta y_\alpha \tag{12}$$

and z_i are the roots of the quartic equation

$$\prod_{i=1}^{4}(z - z_i) = z^4 + y_\alpha y_D z^3 + (y_\gamma + y_\beta + y_\delta y_\alpha) z^2 + y_\alpha y_D y_\gamma z + y_\alpha y_\delta y_\gamma = 0 \tag{13}$$

The roots can be found in closed algebraic form by standard procedures such as that described in Section 3.8.3 of the handbook of Abramowitz and Stegun [31]; in that case, the first two roots are typically real and the final two roots are complex conjugates. The expression in Eq. (11) is real, although the arguments may be complex. Our definition of the z_i differs by a minus sign from that published in Refs. 25, 27, and 29.

The final term Ω_0 in Eq. (8) represents the contribution of dynamical fluctuations to the thermal conductivity, which is caused by the long-time tail of their correlations [25–28]. This term must be subtracted in Eq. (8) so that the experimental thermal conductivity well away from the critical region can be identified with the background thermal conductivity; these contributions are thus included in the background correlation rather than in the enhancement term described by Eq. (8). We have retained the empirical term proposed by Olchowy and Sengers [25–28] but have

slightly revised the denominator appearing in Ω_0. The term Ω_0 is defined by

$$\Omega_0 = \frac{2\left\{1 - \exp\left[\dfrac{-q_D\xi}{1+(q_D^3\xi^3\rho_c^2/3\rho^2)}\right]\right\}}{\pi\left[1 + y_\alpha y_D + \dfrac{y_\beta}{(1+y_\gamma)}\right]} \tag{14}$$

The term Ω_0 rigorously cancels Ω to lowest order in an expansion about $q_D\xi = 0$, that is, well away from the critical point. We have removed the term in the denominator of Ω_0 which does not explicitly contribute to the term cancellation; other higher-order terms remain in the exponential and the denominator. Our revision of Ω_0 has only a small effect on the enhancement calculated from Eq. (8) since its contribution is important only to points far from the critical point where the total enhancement is negligible.

We chose values for the universal and fluid-dependent parameters as indicated above: $R_c = 1.01$, $\nu = 0.63$, $\gamma = 1.2415$, $T_c = 150.6633$ K, $\rho_c = 13.29$ mol · L^{-1}, $P_c = 4.860$ MPa, $\Gamma = 0.075$, and $\xi_0 = 0.16$ nm. With $T_r = 2.5T_c$ we will find the optimum value for q_D^{-1} which satisfies both our critical enhancement data and the data of Trappeniers [12], which are much closer to the critical temperature. This optimum value is found to be $q_D^{-1} = 0.200$ nm. The calculated thermal conductivity critical enhancement along the critical isochore from this function is plotted along with the available experimental data from Refs. 5, 12, 32, and 33 in Fig. 3. Devia-

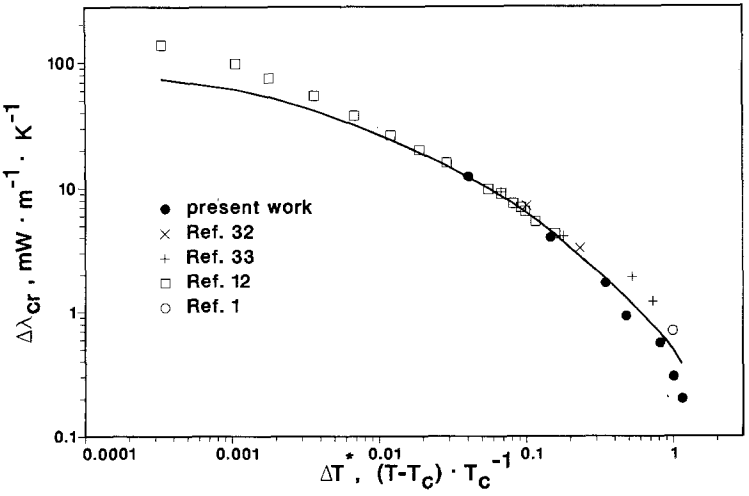

Fig. 3. The variation of $\Delta\lambda_{cr}$ with reduced temperature $\Delta T^* = (T - T_c)/T_c$ along the critical isochore. Line is given by Olchowy and Sengers [25], with $q_D^{-1} = 0.200$ nm and $T_r = 2.5T_c$.

tions between the calculated critical enhancement and the Trappeniers [12] data at temperatures within 1 K of the critical temperature are probably due to the use of the classical equation of state of Stewart and Jacobsen [9] to evaluate the critical enhancement using the Olchowy-Sengers theory.

6. THERMAL CONDUCTIVITY SURFACE

We have demonstrated above that the theoretically based expressions for λ_0 and λ_1 are in good agreement with our thermal conductivity data for argon. Adopting the traditional technique of breaking the thermal conductivity into three terms, we have

$$\lambda = \lambda_0(T) + \lambda_{ex}(T, \rho) + \Delta\lambda_{cr}(T, \rho) \tag{15}$$

We first look at the thermal conductivity surface we developed in Ref. 5 and then develop the new surface. To make the comparison consistent, we substitute the corrected data and we use the $\lambda_0(T)$ function of Kestin et al. [10] with our empirical surface of Ref. 5. The uncertainty in the thermal conductivity surface at 95% confidence is $\pm 3.4\%$, with large deviations in the vapor and liquid isotherms close to the critical temperature. A plot of the deviations for this conductivity surface is given in Fig. 4. Even though λ_{ex} is a function of both temperature and density, we

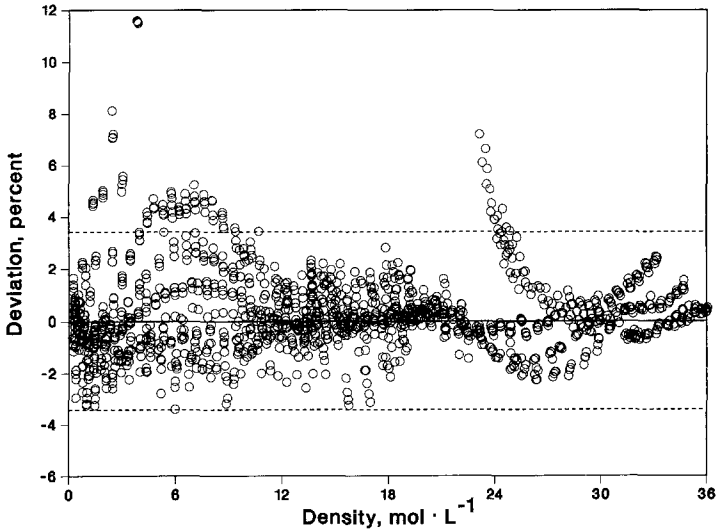

Fig. 4. Deviations between our experimental thermal conductivity data and the correlation, $\lambda = \lambda_0 + \lambda_{ex} + \Delta\lambda_{cr}$, where λ_0 is from Kestin et al. [10] and where λ_{ex} and $\Delta\lambda_{cr}$ are empirical as given in our previous correlation [5].

can distinguish individual isotherms on this deviation plot at liquid densities.

We now turn to the new surface, where we use the function of Kestin et al. [10] for $\lambda_0(T)$ and the function of Olchowy and Sengers [25], with $T_r = 2.5$ and $q_D^{-1} = 0.200$ nm, for $\Delta\lambda_{cr}(T, \rho)$. In addition, we use the results on the first density coefficient of the thermal conductivity by Rainwater and Friend [21, 22] as follows. Table II shows that the $\lambda_1(T)$ function of Rainwater and Friend [22, 23], as well as the experimentally obtained values, is very nearly temperature independent, with an average value of $1.06\ \mathrm{mW \cdot L \cdot mol^{-1} \cdot m^{-1} \cdot K^{-1}}$. We assume λ_{ex} to be temperature independent over the range of our data. We next propose a simple polynomial in density for the thermal conductivity excess function,

$$\lambda_{ex} = \alpha_1 \rho + \alpha_2 \rho^2 + \alpha_3 \rho^3 + \alpha_4 \rho^4 \tag{16}$$

In general, the coefficients α_i could be functions of temperature, but we assume that they are temperature independent. The term α_1 is the first density coefficient of thermal conductivity. These four coefficients in Eq. (16) will be selected to minimize errors between our experimental thermal conductivity data and the surface of Eq. (15). The four optimized coefficients are

$$\begin{aligned} \alpha_1 &= \ \ 0.757\ 894 \times 10^{-3} \\ \alpha_2 &= \ \ 0.612\ 624 \times 10^{-4} \\ \alpha_3 &= -0.205\ 353 \times 10^{-5} \\ \alpha_4 &= \ \ 0.745\ 621 \times 10^{-7} \end{aligned}$$

where ρ is in $\mathrm{mol \cdot L^{-1}}$ and λ_{ex} is in $\mathrm{W \cdot m^{-1} \cdot K^{-1}}$. Deviations between our data and the resulting fit are shown in Fig. 5. The deviations in Fig. 5 are $\pm 2.2\%$ at the 2-sigma confidence interval. The agreement is quite good, especially considering that it covers the liquid, vapor, and supercritical gas phases. Only five adjustable parameters have been used in the development of this thermal conductivity surface. These parameters are q_D^{-1} in the mode-coupling critical enhancement function and the four α_i coefficients in the excess function. The deviations along the near-critical temperature liquid and vapor isotherms which are so pronounced in Fig. 4 are not present in Fig. 5.

We have not constrained the coefficient α_1 to be equal to the average theoretical value of λ_1 which is predicted by Rainwater and Friend [22]. Nor is it possible to do so. Given the form of Eqs. (8) and (16), there must be two contributions to the first term in density, one from the thermal

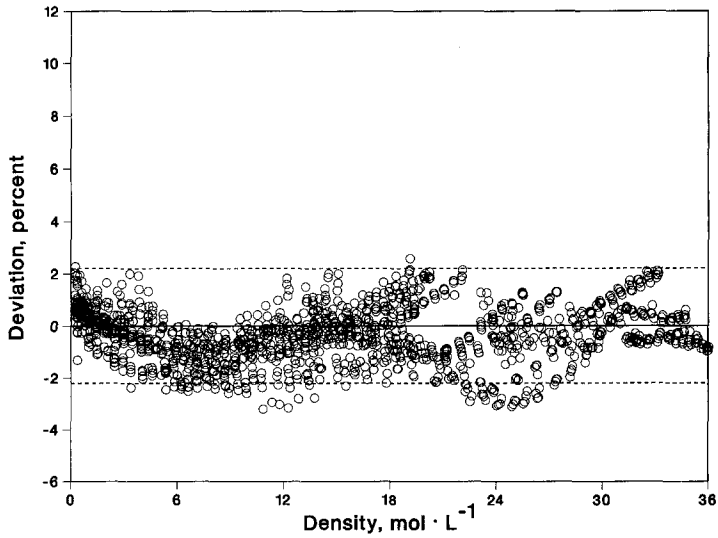

Fig. 5. Deviations between our experimental thermal conductivity data and the new correlation, $\lambda = \lambda_0 + \lambda_{ex} + \Delta\lambda_{cr}$, where λ_0 is from Kestin et al. [10]. λ_{ex} is taken to be temperature independent, based on the first density coefficient theory of Rainwater and Friend [21, 22], and is defined by Eq. (16), while $\Delta\lambda_{cr}$ is from Olchowy and Sengers [25].

conductivity excess function and one from the critical enhancement. Thus, even when a thermal conductivity surface is developed using as strong a theoretical basis as we have in this paper, ambiguities in the determination of the thermal conductivity excess function remain.

7. CONCLUSIONS

In our previous paper [5], we recommended that a new effort be undertaken to correlate the thermal conductivity of argon at low temperatures. This paper presents the results of such an effort. Recent theoretical expressions for $\lambda_0(T)$ and $\lambda_1(T)$ allowed us to detect an error in our data analysis procedure which affected the argon data at densities below 5 mol · L^{-1}. This error arises from an incorrect volume in the fluid compression-work correction. When corrected, our low-density argon heat capacities are in much better agreement with values calculated from the Younglove equation of state [8], confirming a better heat balance on our transient hot-wire system. Thus, we may use thermal diffusivity as a cross check of the reliability of thermal conductivity data, even at low densities.

Our corrected low-density thermal conductivity data are in very good

agreement with the function for $\lambda_0(T)$ of Kestin et al. [10] and the function for $\lambda_1(T)$ of Rainwater and Friend [21, 22]. In addition, when we consider all of our data, we find that the function for $\Delta\lambda_{cr}(T, \rho)$ of Olchowy and Sengers [25] is a good representation for the critical enhancement. Using these theoretically based functions we can optimize the thermal conductivity excess function to produce a much improved thermal conductivity surface. The uncertainty for the new surface at a 95% condidence interval is $\pm 2.2\%$. The surface provides an accurate representation of our argon data from 100 to 324 K in the liquid, vapor, and supercritical regions.

A copy of the computer program which generates the low-temperature argon thermal conductivity surface may be obtained by writing to R. A. Perkins.

ACKNOWLEDGMENTS

We thank Arno Laesecke for many helpful discussions concerning his wide-range correlations of the transport properties of nitrogen and oxygen and the magnitude of errors associated with assuming a temperature-independent thermal conductivity excess function. D. G. Friend gratefully acknowledges financial support from the United States Department of Energy, Division of Chemical Sciences, Office of Basic Energy Sciences.

REFERENCES

1. C. A. Nieto de Castro and H. M. Roder, *J. Res. Natl. Bur. Stand (U.S.)* **86**:293 (1981).
2. C. A. Nieto de Castro and H. M. Roder, in *Proc. 8th Symp. Thermophys. Prop.*, J. V. Sengers, ed. (ASME, New York, 1982), Vol. I, p. 241.
3. J. C. G. Calado, U. V. Mardolcar, C. A. Nieto de Castro, H. M. Roder, and W. A. Wakeham, *Physica* **143A**:314 (1987).
4. H. M. Roder, C. A. Nieto de Castro, and U. V. Mardolcar, *Int. J. Thermophys.* **8**:521 (1987).
5. H. M. Roder, R. A. Perkins, and C. A. Nieto de Castro, *Int. J. Thermophys.* **10**:1141 (1989); H. M. Roder, R. A. Perkins, and C. A. Nieto de Castro, Natl. Inst. Stand. Tech. (U.S.) Interagency Rep. 88-3902, Oct. (1988).
6. J. J. Healy, J. J. de Groot, and J. Kestin, *Physica* **82C**:392 (1976).
7. C. A. Nieto de Castro, B. Taxis, H. M. Roder, and W. A. Wakeham, *Int. J. Thermophys.* **9**:293 (1988).
8. B. A. Younglove, *J. Phys. Chem. Ref. Data* **11**:Suppl. 1 (1982).
9. R. B. Stewart and R. T. Jacobsen, *J. Phys. Chem. Ref. Data* **18**:639 (1989).
10. J. Kestin, K. Knierim, E. A. Mason, B. Najafi, S. T. Ro, and M. Waldman, *J. Phys. Chem. Ref. Data* **13**:229 (1984).
11. B. A. Younglove and H. J. M. Hanley, *J. Phys. Chem. Ref. Data* **15**:1323 (1986).
12. N. J. Trappeniers, in *Proc. 8th Symp. Thermophys. Prop.*, J. V. Sengers, ed. (ASME, New York, 1982), Vol. I, p. 232.

13. V. A. Rabinovich, A. A. Vasserman, V. I. Nedostup, and L. S. Veksler, in *Thermophysical Properties of Neon, Argon, Krypton, and Xenon*, T. B. Selover, Jr., ed. (Hemisphere, Washington, D.C., 1988), p. 203.
14. J. Kestin, R. Paul, A. A. Clifford, and W. A. Wakeham, *Physica* **100A**:349 (1980).
15. M. J. Assael, M. Dix, A. Lucas, and W. A. Wakeham, *J. Chem. Soc. Faraday Trans.* **77**:439 (1981).
16. A. A. Clifford, P. Gray, A. I. Johns, A. C. Scotts, and J. T. R. Watson, *J. Chem. Soc. Faraday Trans.* **77**:2679 (1981).
17. E. N. Haran, G. C. Maitland, M. Mustafa, and W. A. Wakeham, *Ber. Bunsenges Phys. Chem.* **87**:657 (1983).
18. U. V. Mardolcar, C. A. Nieto de Castro, and W. A. Wakeham, *Int. J. Thermophys.* **7**:259 (1986).
19. J. Millat, M. Mustafa, M. Ross, W. A. Wakeham, and M. Zalaf, *Physica* **145A**:461 (1987).
20. J. Millat, M. J. Ross, and W. A. Wakeham, *Physica* **159A**:28 (1989).
21. D. G. Friend and J. C. Rainwater, *Chem. Phys. Lett.* **107**:590 (1984).
22. J. C. Rainwater and D. G. Friend, *Phys. Rev. A* **36**:4062 (1987).
23. C. A. Nieto de Castro, D. G. Friend, R. A. Perkins, and J. C. Rainwater, *Chem. Phys.* **145**:19 (1990).
24. J. V. Sengers, R. S. Basu, and J. M. H. Levelt Sengers, NASA Contractor Report No. 3424 (1981).
25. G. A. Olchowy and J. V. Sengers, *Phys. Rev. Lett.* **61**:15 (1988).
26. G. A. Olchowy and J. V. Sengers, *Int. J. Thermophys.* **10**:417 (1989).
27. G. A. Olchowy and J. V. Sengers, *Representative Equations for the Transport Properties of Carbon Dioxide in the Critical Region*, University of Maryland Technical Report BN 1052 (College Park, MD., 1986).
28. G. A. Olchowy, *Crossover from Singular to Regular Behavior of the Transport Properties of Fluids in the Critical Region*, Ph.D. thesis (University of Maryland, College Park, 1989).
29. R. Mostert, H. R. van den Berg, P. S. van der Gulik, and J. V. Sengers, *J. Chem. Phys.* **92**:5454 (1990).
30. R. A. Perkins, H. M. Roder, D. G. Friend, and C. A. Nieto de Castro, *Physica A* **173**:332 (1991).
31. M. Abramowitz and I. A. Stegun, *Handbook of Mathematical Functions*, Applied Mathematics Series 55 [National Bureau of Standards (U.S.), 1972], pp. 17–18.
32. B. J. Bailey and K. Kellner, *Physica* **31**:444 (1968).
33. L. D. Ikenberry and S. A. Rice, *J. Chem. Phys.* **39**:156 (1963).